

SPECTROSCOPY WITH LARGE  $\gamma$ -ARRAYS  
IN COINCIDENCE WITH A RFD\*K. SPOHR<sup>1</sup>, W. MĘCZYŃSKI<sup>2</sup>, J.B. FITZGERALD<sup>1</sup>, D.B. FOSSAN<sup>5</sup>M. GÓRSKA<sup>3</sup>, H. GRAWE<sup>1</sup>, J. GRĘBOSZ<sup>2</sup>, J. HEESE<sup>1</sup>, M. JANICKI<sup>2</sup>M. LACH<sup>2</sup>, K.H. MAIER<sup>1</sup>, A. MAJ<sup>2</sup>, J.C. MERDINGER<sup>4</sup>M. PALACZ<sup>6</sup>, M. REJMUND<sup>3</sup>, R. SCHUBART<sup>7</sup> AND J. STYCZEŃ<sup>2</sup><sup>1</sup> Hahn-Meitner-Inst., D-14109 Berlin, Germany<sup>2</sup> Institute of Nuclear Research, 31-342 Kraków, Poland<sup>3</sup> Warsaw University, Hoża 69, 00-681 Warszawa, Poland<sup>4</sup> CRN, F-67037 Strasbourg, France<sup>5</sup> SUNY Stony Brook, NY 11794, USA<sup>6</sup> Royal Inst. of Technology, S-10044 Stockholm, Sweden<sup>7</sup> HMI Berlin and University of Göttingen, D-3400 Göttingen, Germany*(Received February 10, 1995)*

A detector (RFD) has been developed that measures evaporation residues in coincidence with  $\gamma$ -rays detected in a Ge-array. Evaporation residues are distinguished by time of flight from any other reaction products with different velocity, like from fission and reactions with light target impurities, and the background from these processes is eliminated. Also the energy of the  $\gamma$ -rays can be Doppler corrected event by event with the measured velocity vector of the emitting nucleus improving the resolution. Recent results of experiments with OSIRIS at VICKSI on  $^{189}\text{Pb}$  and nuclei around doubly magic  $^{56}\text{Ni}$ , that show the performance of the detector, are presented and the perspectives of the RFD application with EUROBALL are discussed.

PACS numbers: 27.40.+z, 27.70.+q, 29.30.Kv, 29.40.Ym

---

\* Presented at the XXIX Zakopane School of Physics, Zakopane, Poland  
September 5-14, 1994.

## 1. Introduction

In beam  $\gamma$ -spectroscopy mostly uses fusion-evaporation reactions to produce the nuclei, that are to be studied. For heavy nuclei and very high spins fission of the compound nucleus dominates over evaporation. The production cross section for evaporation residues can then become so small that also other processes like Coulomb excitation are much stronger. In these cases it is helpful or even necessary to distinguish  $\gamma$ -rays from fusion-evaporation reactions by an ancillary detector from the other processes. This can be accomplished by detecting evaporation residues that recoil out of a thin target in coincidence with the  $\gamma$ -rays. The majority of the recoiling nuclei emerges in a narrow forward cone and is not separated from the many orders of magnitude more abundant scattered beam particles. Therefore, so far, ion optical systems have been used behind the target to separate recoiling nuclei from scattered beam. Recoil mass separators achieve this with high perfection and in addition determine  $A$  and sometimes  $Z$  of the produced nucleus. The idea of the scheme described here is instead, to use a very fast detector that tolerates many scattered beam particles and therefore needs only little separation between beam and recoiling nuclei. Besides selecting the wanted events from the background the velocity vector of the  $\gamma$ -emitting nucleus is also measured and consequently the Doppler shift of the measured  $\gamma$ -rays can be corrected event by event.

Such a detector (recoil-filter detector, RFD) has been designed and built jointly by IFJ Kraków and HMI Berlin, and has been used [1] with the OSIRIS array [2] at VICKSI. It has been described in Ref. [3]. Based on these experiences a modified version for EUROGAM at Strasbourg has been built by a Kraków-Strasbourg-Berlin cooperation. The basic features of the RFD, the experiences from the experiments performed so far and the anticipated use with EUROBALL are discussed in the following.

## 2. The detector

Only a short description of the detector is given here, Ref. [3] gives details. Evaporation residues are distinguished by their slow velocity from scattered beam and other reaction products, particularly fission products. The velocity is measured by time of flight at a distance of 73 cm at OSIRIS and 128 cm at EUROBALL. The detector is composed of 18 identical cylindrical elements, that cover the range from  $2.7^\circ$  to  $12.1^\circ$  (OSIRIS) and  $1.4^\circ$  to  $6.7^\circ$  (EUROBALL) with 65% geometrical efficiency. Fig. 1 shows the general layout for EUROBALL. The individual detector elements are arranged in two concentric rings of 6 elements (inner ring) and 12 elements (outer ring). Each element consists of a thin (0.5 to 2  $\mu\text{m}$ ) aluminized mylar

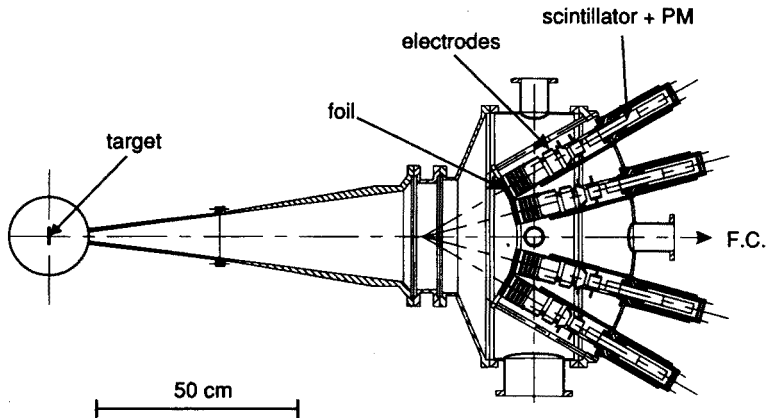


Fig. 1. Layout of the RFD for EUROBALL at Strasbourg. 18 identical elements are arranged around a central hole for the beam, they cover the range from  $1.4^\circ$  to  $6.7^\circ$  with a geometrical efficiency of 65%; this design fits into EUROBALL with all  $\gamma$ -detectors. The elements are tilted away from the axis, so that scattered beam cannot directly hit the scintillators. The flightpath is 128 cm.

foil; ions hitting the foil knock out electrons. These electrons are accelerated by 20 kV and focussed onto a thin, fast plastic scintillator (Fig. 2). As the electrons from one ion hit the scintillator simultaneously ( $\Delta t \simeq 0.1$  ns), they produce a summed signal of  $20 \text{ kV} \times \text{number of electrons}$  (typically  $20 \text{ kV} \times 100 = 2 \text{ MeV}$ ). The number of emitted electrons is proportional to the electronic energy loss of the ions [4] and therefore the signal height for very slow heavy nuclei as 10 MeV Pb is sizeable, *e.g.* comparable to that of scattered beam. A pulsed beam with a typical repetition rate of 3 Mc/s is used; all scattered beam particles that hit the detector arrive then at the same time and fast linear gates prevent these pulses to reach the following electronics. In coincidence with  $\gamma$ -rays the time of flight of the detected ion and the number of the detector element that has been hit are measured and stored. This defines the magnitude and the angle of the velocity vector of the nucleus, that has emitted the  $\gamma$ -ray.

### 3. Recent results and detector performance

#### $^{189}\text{Pb}$

Following the finding [1] that deformed bands become yrast already from the  $4^+$ -state on in  $^{186,188}\text{Pb}$  it is of interest, if the unpaired  $i_{13/2}$  neutron in the odd Pb-isotopes favours the deformed or spherical shape. Spectroscopy of  $^{187,189}\text{Pb}$  has been attempted with the  $^{155,157}\text{Gd}(^{36}\text{Ar}, 4n)$ -reaction at 173 MeV. The cross section of these reactions is however so

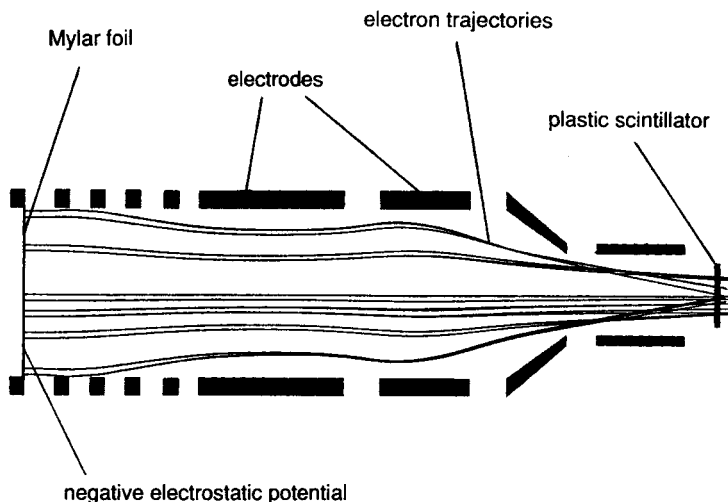


Fig. 2. The RFD-element for EUROBALL. Electrons emitted from the aluminized mylar foil are accelerated by the electrode structure along the indicated trajectories to the scintillator. The design of the last electrodes has been changed from the OSIRIS version to still improve the focussing of the electrons onto the scintillator. The diameter of the foil is 6 cm.

low that only marginal data could be gained for  $^{189}\text{Pb}$ . Fig. 3 shows the calculated energy and angular distribution of the  $^{189}\text{Pb}$  recoils from this reaction. In this case the distribution of the recoils due to the evaporation of neutrons is so narrow that the recoils are not separated from the beam. But angular straggling in the  $1\text{ mg/cm}^2$  target scatters about 50% into the sensitive range of the detector and separates them partly from the beam, that scatters less ( see also Fig. 7). The suppression of fission and Coulex by the RFD-coincidence requirement gives clearly resolved lines already in a singles- $\gamma$ -spectrum (Fig. 4). The remaining intensity of the Coulex lines is due to random coincidences. Most of the lines in Fig. 4 are known in neighbouring nuclei. But from RFD- $\gamma\gamma$  and RFD- $\gamma$ -X coincidences a tentative scheme for  $^{189}\text{Pb}$  could be derived (Fig. 5). The comparison with the scarce data on neighbouring Pb-isotopes (Fig. 5) suggests that  $^{189}\text{Pb}$  is spherical.

### Nuclei around $^{56}\text{Ni}$

The nuclei around doubly magic  $^{56}\text{Ni}$  have gained much interest recently. One expects close similarities to  $^{100}\text{Sn}$ , as the shell gap is in both cases between spin-orbit partners, namely  $f_{7/2}$  and  $f_{5/2}$  or  $g_{9/2}$  and  $g_{7/2}$  resp. and both nuclei have  $N = Z$ . Also very much energy is required to gain angular momentum with shell model states around  $^{56}\text{Ni}$ , so that nonspherical shapes might compete.

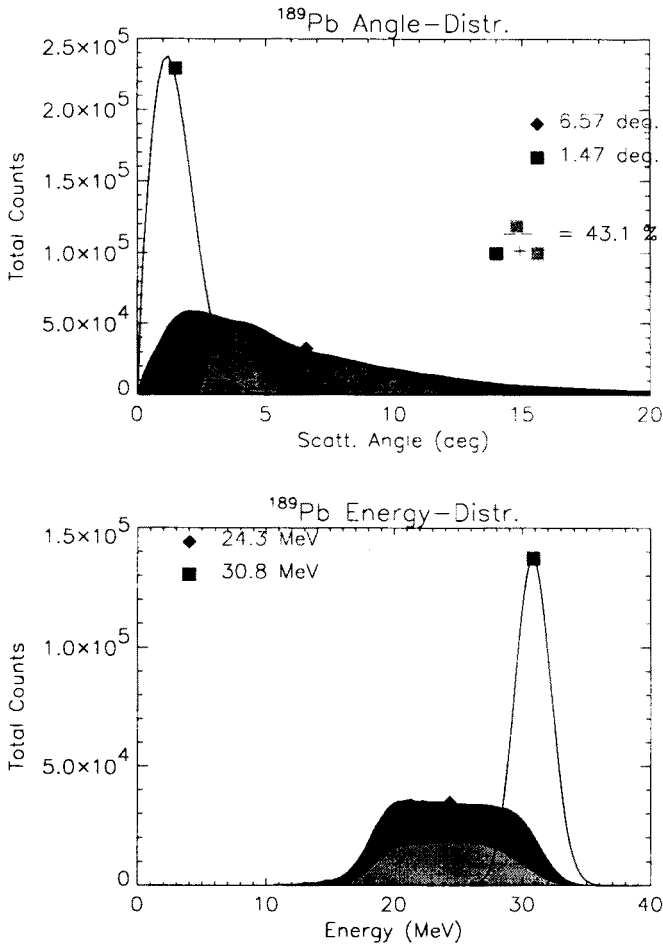


Fig. 3. Calculated angular and energy distribution of  $^{189}\text{Pb}$  from the reaction  $^{157}\text{Gd}(^{36}\text{Ar}, 4n)^{189}\text{Pb}$  at 173 MeV with a 1 mg/cm<sup>2</sup> target. The lines show the distributions resulting only from particle evaporation. The dark shaded area includes in addition the passage of the nuclei through the target. The fraction of nuclei hitting the sensitive area of the detector are shown by the light shade, which is 43.1% in this case. The centroids of the distributions are also indicated.

An experiment with a 68 MeV  $^{20}\text{Ne}$  beam on a 1mg/cm<sup>2</sup>  $^{40}\text{Ca}$ -target has been performed to study nuclei around  $^{56}\text{Ni}$ . In this case fusion-evaporation reactions dominate and the main role of the RFD is to improve the  $\gamma$ -energy resolution. Fig. 6 shows the calculated energy and angular distribution for  $^{54}\text{Fe}$  following the evaporation of one  $\alpha$ -particle and two protons and the subsequent energy loss and straggling in the target. Evaporation of a particle with mass  $A_p$  and energy  $E_p$  changes the velocity of the

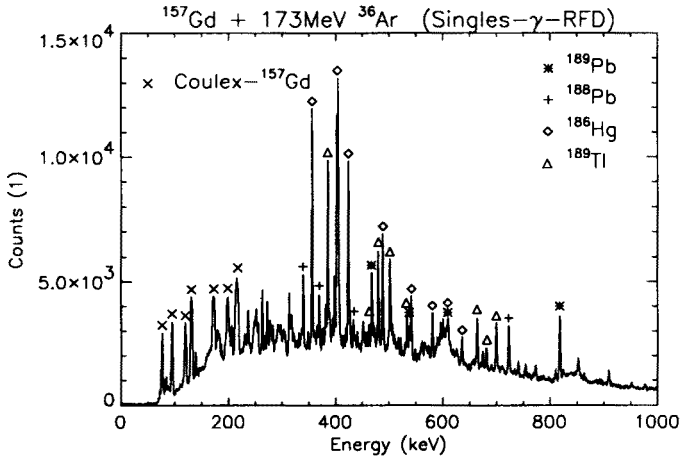


Fig. 4.  $\gamma$ -spectrum (singles) from the reactions of 173 MeV  $^{36}\text{Ar}$  with a 1 mg/cm<sup>2</sup>  $^{157}\text{Gd}$ -target.

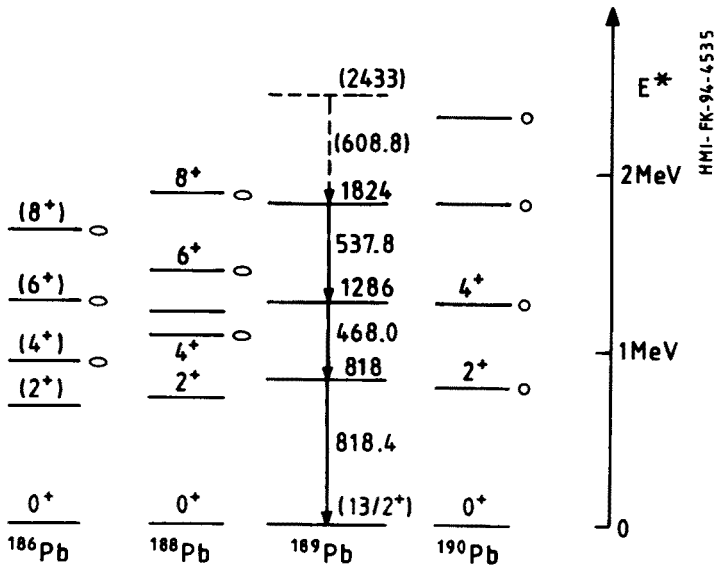


Fig. 5. Tentative level scheme of  $^{189}\text{Pb}$  in comparison with the neighbouring nuclei, showing close similarity to spherical  $^{190}\text{Pb}$  (O) but not to the deformed states of  $^{188,186}\text{Pb}$  (□).

nucleus with mass  $A_N$  by  $\Delta v/c \simeq 0.05\text{MeV}^{-1/2} \sqrt{E_p A_p/A_N}$ . This change of velocity is isotropic, if particle emission is isotropic, and its distribution therefore gives equal Doppler broadening at all angles and is independent of

the mean velocity of the nucleus. The linewidth is  $\Delta E_\gamma/E_\gamma \geq 1\%$  (fwhm) for  $^{54}\text{Fe}$  due to this effect in the present case. A correction is only possible by measuring the velocity of the nucleus as with the RFD or by measuring the evaporated particles. The other important contribution to the Doppler broadening in this experiment is the variation of the energy loss due to the target thickness, which could be minimized by using a thinner target. The RFD measures the velocity of the nucleus after it has left the target. Usually the flight time of the nuclei through the target is a few tenths of a picosecond and  $\gamma$ -rays are emitted behind the target and therefore Doppler corrected in the right way. But in the present case with the  $1\text{ mg/cm}^2$  Ca-target this time can become  $1\text{ ps}$  and for the fastest transitions, that occur still inside the target, wider lines than expected are found due to a partly wrong correction.

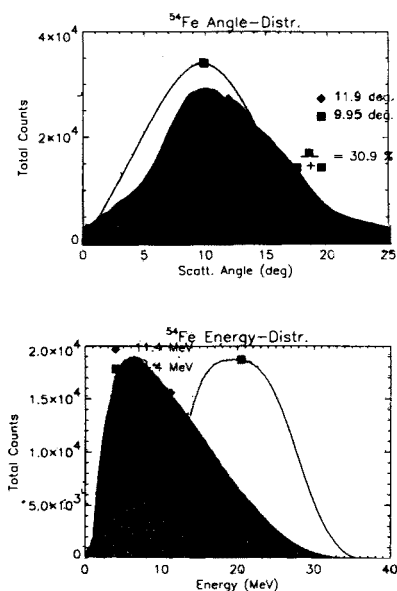


Fig. 6. Calculated angular and energy distribution of  $^{54}\text{Fe}$  from the reaction  $^{40}\text{Ca}(^{20}\text{Ne}, \alpha 2p)^{54}\text{Fe}$  at 68 MeV with a  $1\text{ mg/cm}^2$  target. See Fig. 3 for further explanations.

Fig. 7 shows the angular distribution of the scattered beam as calculated with TRIM [5]. This distribution means that each inner RFD-element was hit by  $\simeq 3$  scattered beam particles per beam pulse for the experimental conditions of 7000 particles per beam pulse at a rate of 3 Mc/s beam pulses. Nevertheless the detector recovered in time to detect the fastest evaporation residues that arrive 50 ns later.

Fig. 8 shows the 2290 keV line from  $^{40}\text{Ca}(^{20}\text{Ne}, 3p)^{57}\text{Co}$ . Its width is reduced from 20 keV fwhm with the usual correction for the average recoil

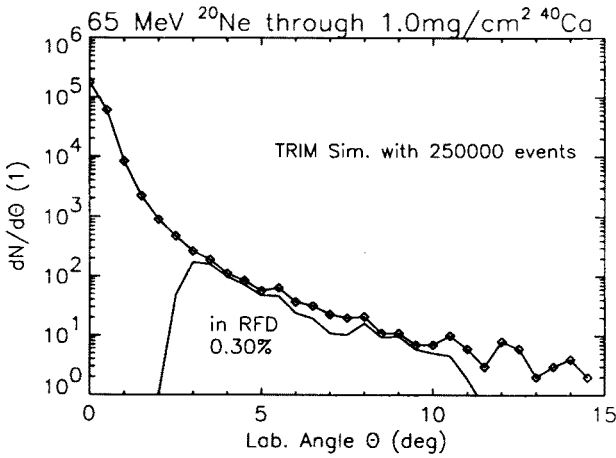


Fig. 7. Angular distribution of 65 MeV  $^{20}\text{Ne}$  after passing through 1 mg/cm<sup>2</sup>  $^{40}\text{Ca}$ . The part of the distribution that hits the sensitive area of the RFD (0.3%) is also shown.

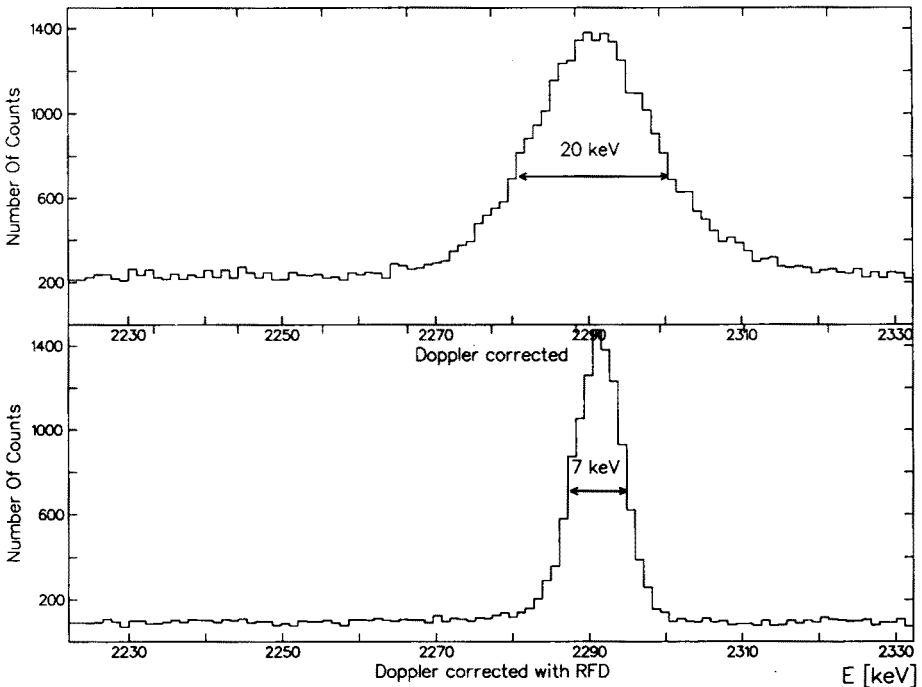


Fig. 8. Part of a  $\gamma\gamma$ -coincidence spectrum showing the 2290 keV line in  $^{57}\text{Co}$  with and without RFD-coincidences, see text.

velocity to 7 keV with the event by event correction for the actual measured velocity. With a thinner target a part of the broadening could have been



avoided, but this rolled target was remarkably clean and free of oxygen. The intensity ratio of the two lines gives the efficiency of the RFD as 30%, but the peak height stays constant, the loss of counts is entirely due to the reduced width. The background is reduced to 30% also simply by the efficiency; as fusion-evaporation is dominant in this case, no real reduction of the background can be expected from the RFD-coincidence requirement.

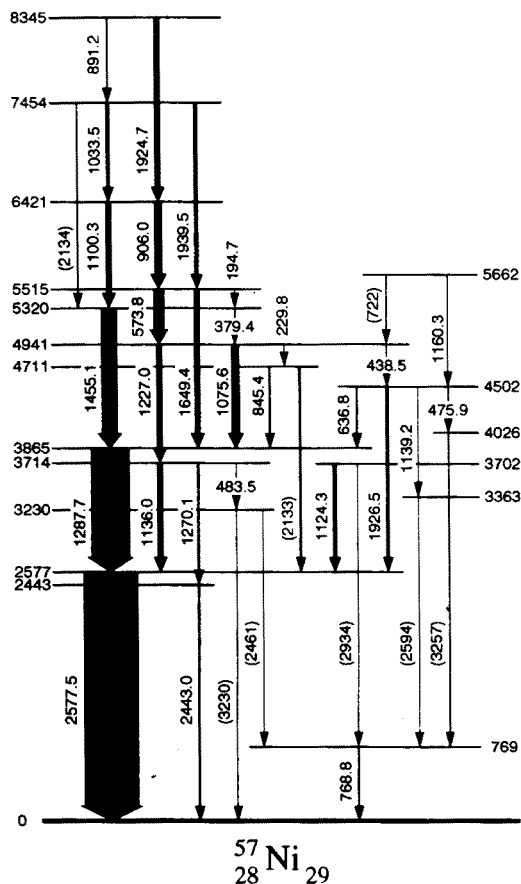


Fig. 9. Provisional level scheme of  $^{57}\text{Ni}$ .

The measured total efficiencies and ratios of outer to inner ring countrate (in parentheses) of the RFD for different final nuclei in this experiment were:  $^{58}\text{Ni}(2p)$  31% (0.41),  $^{57}\text{Ni}(2pn)$  30% (0.49),  $^{57}\text{Co}(3p)$  30% (0.50),  $^{56}\text{Fe}(4p)$  38% (0.53),  $^{54}\text{Fe}(\alpha 2p)$  28% (1.02). This loss of countrate over pure  $\gamma\gamma$ -coincidences is clearly outweighed by the improved resolution. The good agreement between measured 28% and calculated 31% efficiency (Fig. 6) for  $^{54}\text{Fe}$  might be fortuitous, as the calculation gives the countrate ratio of outer

to inner ring as 2. The calculations depend on some unproven assumptions, as isotropic particle evaporation and constant cross section throughout the target; therefore quantitative agreement cannot be expected.

The big improvement in resolution allows now to study high spin states in these nuclei much better. A preliminary level scheme of  $^{57}\text{Ni}$  from the present experiment is shown in Fig. 9. It shows the irregular structure of a shell-model nucleus. To gain one unit of angular momentum nearly 1 MeV is needed, and the high energies of the  $\gamma$ -transitions imply, that Doppler broadening determines the resolution.

#### 4. Perspectives for an RFD with the new $\gamma$ -arrays

The RFD has been developed into a reliable instrument in the experiments with OSIRIS at VICKSI, particularly the difficulties with the very high countrates from scattered beam have been solved. The remaining open problem is that in most experiments the measured efficiency was around 30% lower than the expectation, that it should be the full geometric efficiency. From the experiences gained so far the perspectives of a RFD with the new much more efficient  $\gamma$ -detector arrays will be discussed below. A second RFD for EUROBALL at Strasbourg has been built and work on a proposal of a RFD for GAMMASPHERE is under way. The following general points have to be kept in mind:

- The RFD is a velocity filter for reaction products under forward angles. Usually slow evaporation residues are selected from faster fission products, reaction products from light target impurities, Coulex *etc.* For high velocities of the CM-system the velocity distributions might overlap.
- The scattered beam gives a lower limit of the detection angle typically at around  $2^\circ$  to  $3^\circ$ .
- The ions to be detected have to pass through the electron emitting foil, this poses an energy limit of about 5 MeV for heavy nuclei.

The results for  $^{189}\text{Pb}$  presented here and for  $^{199}\text{At}$  [6] show that clean spectra can be filtered out of a 100 to 1000 times larger background. The cross section for  $^{199}\text{At}$  has been estimated from the experiment as  $\simeq 0.1$  mb, while the calculated total reaction cross section is 100 mb. EUROBALL at Strasbourg has about the same efficiency for  $\gamma\gamma$ -coincidences as OSIRIS for a single  $\gamma$  or 100 times the  $\gamma\gamma$ -efficiency of OSIRIS. Therefore for  $^{189}\text{Pb}$  one can expect the statistics of Fig. 4 in a  $\gamma\gamma$ -cut on a single line. Nuclei with a production cross section of  $\simeq 10\mu\text{b}$  will become accessible for spectroscopy.

The Doppler correction for the velocity distribution of the recoils becomes more important in two respects with the new arrays. The smaller opening angle of the individual Ge-detectors decreases the corresponding

contribution to the Doppler width and consequently the velocity distribution of the recoils becomes more significant. Also higher fold (f)  $\gamma$ -coincidences are measured and the resolving power of the array is  $\sim \Delta E_{\gamma}^f$ .

An instructive comparison is between  $\gamma^f$ -RFD and  $\gamma^{f+1}$ -coincidences. The efficiency of the RFD at Strasbourg will be  $\geq 15\%$ , roughly twice the photopeak efficiency of EUROBALL. Therefore, unless multiple gates on  $\gamma$ -lines are used, a gain in the countrate of a factor 2 is achieved. The resolving power of the array increases by roughly a factor 10 with each higher fold. Therefore the RFD is favoured, if fusion is less than 10% of the total cross section and consequently the RFD reduces the background by more than a factor 10, which is clearly the case for the heavy fissile nuclei studied so far. In addition the improvement of the line width has to be considered. For the  $^{56}\text{Ni}$ -experiment this means that  $\gamma^2$ -RFD coincidences with three times improved line width are about equivalent to  $\gamma^3$  coincidences and for higher folds the RFD gives better resolving power due to the  $\Delta E_{\gamma}^f$  dependence. Another point is that the data with the RFD will be more simple and clear and it is therefore more likely that unexpected features will be found.

The RFD occupies very little solid angle ( $\leq 2\%$ ) and does, therefore, not obstruct the  $\gamma$ -measurement or any additional detectors. The detector for EUROBALL works with the complete array. Pure  $\gamma$ -coincidences can be measured unimpeded simultaneously to  $\gamma$ -RFD-coincidences; only a pulsed beam has to be used and the target thickness might be restricted. One can expect that the RFD improves a majority of thin target experiments.

This work has been supported in part through the agreement on scientific cooperation between Poland and Germany and by the Polish State Committee for Scientific Research under grant No 2 P03B 112 08.

## REFERENCES

- [1] J. Heese *et al.*, *Phys. Lett.* **B302**, 390 (1993).
- [2] R.M. Lieder *et al.*, *Nucl. Instrum. Methods* **A220**, 363 (1984).
- [3] J. Heese *et al.*, *Acta Phys. Pol.* **B24**, 61 (1993).
- [4] H. Rothard *et al.*, in *Particle Induced Electron Emission II*, Springer Tracts in Modern Physics, Vol. 123, Springer, 1991.
- [5] J.P. Biersack, L.G. Haggmark, *Nucl. Instrum. Methods* **174**, 257 (1980).
- [6] K. Spohr *et al.* in Proc. of Conf. on Physics from Large  $\gamma$ -ray Detector Arrays, Berkeley, Aug. 1994 and Annual Report 1993, Bereich Schwerionenphysik Hahn-Meitner-Institut, ISSN 0944-0305, p. 54.